ELSEVIER

Mutation Research 473 (2001) 121–136

Fundamental and Molecular Mechanisms of Mutagenesis

www.elsevier.com/locate/molmut
Community address: www.elsevier.com/locate/mutres

Inducible mutagenesis in TEPC 2372, a mouse plasmacytoma cell line that harbors the transgenic shuttle vector λLIZ

K. Felix [a,*], A.L. Kovalchuk [a], S.S. Park [a], A.E. Coleman [a], E.S. Ramsay [a], M. Qian [a], K.A. Kelliher [a], G.M. Jones [a], T. Ried [b], G.W. Bornkamm [c], S. Janz [a]

[a] *Laboratory of Genetics, DBS, NCI, Building 37, Room 2B10, Bethesda, MD 20892-4255, USA*
[b] *Medicine Branch, NCI, NIH, Bethesda, MD, USA*
[c] *Institute of Molecular Biology and Tumor Genetics, GSF, Munich, Germany*

Received 14 September 2000; received in revised form 12 October 2000; accepted 12 October 2000

Abstract

The plasmacytoma cell line, TEPC 2372, was derived from a malignant plasma cell tumor that developed in the peritoneal cavity of a BALB/c mouse that harbored the transgenic shuttle vector for the assessment of mutagenesis in vivo, λLIZ. TEPC 2372 was found to display the typical features of a BALB/c plasmacytoma. It consisted of pleomorphic plasma cells that secreted a monoclonal immunoglobulin (IgG2b/λ), was initially dependent on the presence of IL-6 to grow in cell culture, contained a hyperdiploid chromosome complement with a tendency to undergo tetraploidization, and harbored a constitutively active c-*myc* gene by virtue of a T(6;15) chromosomal translocation. TEPC 2372 was further characterized by the ability to respond to in vitro exposure with 4-NQO (4-nitroquinoline-1-oxide), an oxidative model mutagen, with a vigorous dose-dependent increase in mutagenesis that peaked at a 7.85-fold elevation of mutant rates in λLIZ when compared to background mutant rates in untreated controls. Cotreatment with 4-NQO and BSO (buthionine sulfoximine), a glutathione-depleting compound that causes endogenous oxidative stress, resulted in a 9.03-fold increase in the mutant frequency in λLIZ. These results demonstrated that TEPC 2372, the malignant plasma cell counterpart of the λLIZ-based in vivo mutagenesis assay, may be useful as an in vitro reference point for the further elucidation of oxidative mutagenesis in lymphoid tissues.

Keywords: λLIZ-based transgenic mutagenicity assay; Pristane (2,6,10,14-tetramethylpentadecane); Peritoneal plasmacytomagenesis; BALB/c mice

1. Introduction

The recent development of transgenic shuttle vector-based mutagenesis systems in the mouse and rat has provided exciting new opportunities for the tissue-specific evaluation of mutagenesis in vivo. Several designs have been called into being [1–4], but the most widely used and best validated systems currently available rely on the phage λ vectors, λlacZ [5,6] and λLIZ [7,8], or the plasmid vector, pUR288 [9]. These vectors have been employed

Abbreviations: BSO, buthionine sulfoximine; CGH, comparative genomic hybridization; Chr(s), chromosome(s); c-*myc*, Myc gene; i.p., intraperitoneal; FCS, fetal calf/bovine serum; Myc, Myc protein; 4-NQO, 4-nitroquinoline-1-oxide; PFU(s), plaque forming unit(s); PhIP, 2-hydroxyamino-1-methyl-6-phenylimidazo[4,5-b] pyridine; SKY, spectral karyotyping; SSLP, simple sequence length polymorphism; TEPC, tetramethylpentadecane-induced plasmacytoma; VRC, vanadyl ribonucleoside complex; X-gal, 5-bromo-4-chloro-3-indolyl-β-D-galactopyranoside; X/XO, xanthine/xanthine oxidase

*Corresponding author. Tel.: +1-301-496-2202; fax: +1-301-402-1031.
E-mail address: felixk@dc37a.nci.nih.gov (K. Felix).

0027-5107/01/$ – see front matter
PII: S0027-5107(00)00143-3

successfully in numerous toxicological and biological research applications, but their use in cancer research has been particularly informative because they make it possible to measure somatic mutagenesis in the very tissues in which carcinogenesis occurs (see http://eden.ceh.uvic.ca/bigblue.htm for a nearly complete bibliography on this subject). Of special interest for research on the development of malignant lymphomas and plasmacytomas were studies that demonstrated that the treatment of mice with mutagens at in vivo exposure levels known to provoke lymphomagenesis was indeed associated with elevated mutagenesis in lymphoid tissues. For example, the λLIZ vector was employed to correlate the lymphoma-inducing potency of the compounds 1,3-butadiene [10,11], dimethylbenzoanthracene [12], benzene [13], and ethylnitrosourea [14] with significant increases in mutagenesis in the lymphoid system. Similar correlations between elevated mutagenicity in lymphoid tissues and development of malignant lymphomas were established for the mutagens benzo[a]pyrene [15], ethylnitrosourea [16] and ethyl carbamate [17], using the λlacZ or pUR288 vectors as the read-out systems. The combined results with all three shuttle vectors, λLIZ, λlacZ, and pUR288, suggested that the assessment of mutagenesis in lymphoid tissues may be of tremendous value, not the least because the ability to predict lymphoma development by means of a short-term assay may help to reduce the need for tumor induction studies in vivo.

Permanent lymphoid cell lines that contain transgenic shuttle vectors for the evaluation of mutagenesis offer useful model systems for comparing the mutagenicity under controlled and manipulable in vitro conditions with the mutagenic in vivo response in lymphoid tissues. Such cell lines can be expected to be of considerable benefit when it is desirable to establish the complete dose-response-curve of lymphoma-inducing mutagens prior to their in vivo testing, to characterize known or identify new modulators of mutagenesis that may either enhance or diminish the genotoxic potency of a particular lymphomagenic compound, and to elucidate the molecular mechanisms of mutagenesis, including DNA repair pathways. Here, we describe the first lymphoid tumor cell line that contains a transgenic shuttle vector for mutagenesis, the λLIZ-harboring plasmacytoma TEPC 2372. The line was derived from a pristane-induced plasmacytoma that developed in the peritoneal cavity of a congenic BALB/c.λLIZ mouse. Cytogenetic and molecular analysis showed that TEPC 2372 displayed the typical phenotype of a BALB/c plasmacytoma: it secreted a monoclonal IgG2b/λ immunoglobulin [18], was initially dependent on IL-6 to grow in vitro [19], exhibited a tendency to undergo tetraploidization [20], and harbored a c-*myc*-deregulating chromosomal translocation; in this case a "variant" form, namely the T(6;15) translocation [18]. TEPC 2372 was further characterized in mutagenicity experiments in vitro, in which it responded to the challenge with the oxidative model mutagen, 4-nitroquinoline-1-oxide (4-NQO), with an up to 7.85-fold increase in mutant levels. This finding — taken in conjunction with the results of phage packaging experiments, which showed that the shuttle vector λLIZ can be rescued from the TEPC 2372 genome with an acceptable efficiency of $\sim 8 \times 10^3$ PFUs/μg of genomic DNA — proved that the λLIZ-based mutagenesis assay was completely functional in the tumor line. The λLIZ assay in TEPC 2372 may thus provide a useful in vitro reference point for the evaluation of mutagenicity in lymphoid tissues. Furthermore, it may be helpful for elucidating the mechanisms of mutagenesis under conditions of deregulated c-*myc* expression.

2. Materials and methods

2.1. Establishment of TEPC 2372

TEPC 2372 was derived from a primary plasmacytoma that was induced in the peritoneal cavity of a 4-week-old BALB/c.λLIZ$^{+/-}$ N_5 mouse by three i.p. injections of 0.2 ml pristane (2,6,10,14-tetramethylpentadecane) [21]. Ascitic fluid containing plasmacytoma cells was obtained by paracentesis and centrifuged to secure the cell pellet. The pellet was freed from red cells by lysis in ACK buffer, resuspended in RPMI 1640 medium supplemented with 10% FCS, 50 μM 2-mercaptoethanol, 10 mM glutamine and 10 plasmacytoma units per milliliter (=0.33 ng/ml) IL-6 [19], plated out in 200 μl

Table 1
Mutant frequencies of gene *lac*I in plasmacytoma cell line TEPC 2372

Experiment[a]	Treatment[b]	Concentration	Time[c]	Blue[d]	Total[e]	MF[f]
1	None	–	–	10	1.17	8.56
1	None	–	–	11	1.38	7.99
1	4-NQO	1 μM	2	66	1.22	54.2
1	4-NQO	2 μM	2	32	1.53	20.9
1	PhIP	1 μM	2	62	1.49	41.7
1	PhIP	2 μM	2	72	1.66	43.4
1	X/XO	4 mM/4 units	24	36	1.28	28.1
2	None	–	–	11	7.05	15.6
2	None	–	–	6	3.57	16.8
2	4-NQO	0.10 μM	24	73	7.78	93.8
2	4-NQO	0.25 μM	24	74	7.07	104.6
2	4-NQO	0.50 μM	24	85	6.69	127.1
2	4-NQO	0.75 μM	24	47	4.43	106.1
2	4-NQO	1.00 μM[g]	24	1	<0.01	?
3	None	–	–	8	6.67	12.0
3	4-NQO/BSO	0.10/10 μM	24	47	5.43	86.6
3	4-NQO/BSO	0.25/10 μM	24	58	5.35	108.4
3	4-NQO/BSO	0.50/10 μM	24	33	3.20	103.1
3	4-NQO/BSO	0.75/10 μM[g]	24	1	<0.01	?

[a] Number of experiment.
[b] The following mutagens were added to exponentially growing cells in culture: 4-NQO (4-nitroquinoline-1-oxide), PhIP (2-hydroxyamino-1-methyl-6-phenylimidazo[4,5-b]pyridine) and X/XO (xanthine/xanthine oxidase).
[c] Incubation time (h).
[d] Number of blue mutant plaques.
[e] Number of total plaques (i.e. blue mutant plus colorless wildtype plaques), as multiples of 10^5.
[f] Mutant frequency calculated as ratio of blue to total plaques, as multiples of 10^{-5}.
[g] This concentration resulted in severe toxicity in plasmacytoma cells. The trypan exclusion assay revealed that most of the cells were dead at the end of the experiment; i.e. after the 24 h incubation period in fresh culture medium. Cell death was accompanied by apparent fragmentation of genomic DNA and the failure to package infectious phage particles. This is indicated by the question marks in the last column of the table.

aliquots in a 96-well plate, and incubated at 37°C and 5% CO_2. In the great majority of wells, the tumor cells either died or were overgrown by adherent fibroblast-like cells in the course of 4 weeks of primary culture. The plasmacytoma cells growing in one well could be sufficiently expanded during the subsequent 4–6 weeks to be used in a pilot mutagenicity experiment (see Experiment 1 in Table 1). However, it took 6 additional months of continuous in vitro propagation to stabilize TEPC 2372 as a robust, vigorously growing cell line. These cells were used for the second and third mutagenicity experiment (see Experiments 2 and 3 in Table 1). Both an IL-6 dependent subline and an IL-6 independent subline were established, the latter by gradually weaning the cells from the growth factor. Both sublines can be viably frozen and readily re-cultured using standard procedures.

2.2. Genotyping and immunoglobulin production

To determine the presence of residual C57BL/6 alleles in TEPC 2372, SSLP genotyping was performed with commercially available PCR primer pairs (Research Genetics). A total of 77 markers that covered at least one centromeric, central and telomeric portion of each autosome and the X chromosome were employed. PCR was performed with Taq polymerase from Perkin-Elmer, dNTPs from Boehringer, and the PCT-100 programmable thermocycler from MJ Research. PCR products were fractionated on 8–10% PAGE gels to distinguish the allelomorphic

differences between C57BL/6 and BALB/c. To test the ability of TEPC 2372 to secrete a monoclonal immunoglobulin/paraprotein, the proteins precipitated from the cell culture supernatant were separated with the Paragon™ SPE electrophoresis system (Beckman) to detect an extragradient. The extragradient was further characterized by ELISA using goat-anti-mouse polyclonal antisera specific for the heavy-chain isotypes and light-chain isotypes of the mouse (Southern Biotechnology). Once the isotype of the paraprotein was determined, the amount of paraprotein secreted into the cell culture medium under steady-state conditions (i.e. after the cells seeded into the culture dish had reached the plateau phase with respect to cell number) was estimated by quantitative ELISA using a serial dilution range of the paraprotein contained in the cell culture supernatant.

2.3. Mapping of λLIZ and molecular cytogenetics (SKY, CGH)

Fluorescence in situ hybridization (FISH) was used to map the chromosomal integration site of the transgenic concatamer, λLIZ. Chromosomes were fixed in methanol/acetic acid (3:1 v/v), dropped onto glass slides, and stored at room temperature for 2 weeks. Phage DNA obtained from λLIZ was employed as the FISH probe. The 43 kb probe was nick-translated with rhodamine 110 (Applied Biosystems), precipitated, resuspended in hybridization solution (35% formamide, 1 × SSC, 5% dextran sulphate), denatured at 88°C for 7 min, and allowed to pre-anneal at 37°C for 1 h. Slides were hybridized for 2 days at 37°C and washed in 50% formamide/2 × SSC at 45°C, 0.1 × SSC at 60°C, and 4 × SSC/Tween 20 at 45°C. The chromosomes were counterstained with 4′,6-diamidino-2-phenylindole (DAPI) and embedded in a solution containing the antifading agent, 1,4-phenylenediamine (Sigma). Images were acquired with a cooled charge-coupled device (CCD) camera (CH250, Photometrics, Tucson, AZ) mounted on a Leica DMRBE epifluorescence microscope. The karyotype of TEPC 2372 was determined by spectral karyotyping (SKY) as described elsewhere [22,23]. Putative gene copy number changes present in TEPC 2372 were assessed by comparative genomic hybridization (CGH) as described previously [24].

2.4. Determination of copy number of λLIZ

Quantitative Southern hybridization was performed to determine the copy number of λLIZ in the TEPC 2372 genome. 10 μg of genomic DNA was digested to completion with Apa I (New England BioLabs). DNA preparation and Southern blotting were performed as described previously [25]. Briefly, the DNA was fractionated in 0.7% agarose at 40 constant volts over a 20 h period and then transferred overnight by capillary blotting to the Nytran membrane #77412 from Schleicher and Schuell. The blot was probed with a 545 bp fragment of the *lac*I gene (i.e. the target gene of mutagenesis contained in the λLIZ phage) that was ^{32}P-labeled via nick translation and hybridized overnight using $\sim 2 \times 10^7$ cpm/ml hybridization solution. Final washing was performed with 0.2 × SSC for 5 min. Fragment intensity was determined by autoradiography employing a molecular dynamics phosphorescence storage screen.

2.5. PCR analysis of the T(6;15) translocation

The fine structure of the T(6;15) translocation was detected by PCR and further elucidated by DNA sequencing, building on our past experience of using these methods for analyzing T(12;15) translocations [26,27]. High-fidelity PCR kits (Boehringer) were employed to amplify 500 ng aliquots of genomic DNA obtained from TEPC 2372. A hot-start PCR technique was utilized with the following cycling conditions: 30 cycles of template denaturation at 95°C for 15 s, primer annealing for 20 s at 62°C for primer pair, Pvt-3′/κ-5′, and 20 s at 55°C for primer pair, Pvt-5′/κ-3′, and primer extension at 68°C for 4 min in the first cycle with a progressive prolongation of the extension time by 20 s for each of the subsequent cycles. PCR products were fractionated on agarose gels, stained with ethidium bromide, and gel purified using the Qiagen gel extraction kit. Purified PCR fragments were sequenced directly using the fmol™ cycle-sequencing kit (Promega). To exclude artifacts, all recombinational fragments were PCR amplified and sequenced at least twice. PCR primers Pvt-3′ and κ-5′ were designed with the help of the Oligo 5.0 software (Biosciences). PCR primers Pvt-5′ and κ-3′ were a gift from Dr. Konrad Huppi, NCI. Primer sequences were as follows, 5′–3′: Pvt-3′, gccca tttgt ctatt acggt

ttct; κ-5′, ctttg acgac ttagg ggaag aaaac; Pvt-5′, gaata tccac aggta caa; κ-3′, gtggg atagc agagt tga. Primer sequences begin with positions 1098, 5366, 2542 and 5366 in GeneBank files MUSPVT1a, MMIG25, MMPVT1M and MMIG25, respectively.

2.6. Detection of c-myc RNA

Cytoplasmic total RNA was extracted at room temperature according to the Nonidet P40 method. Briefly, the TEPC 2372 cell pellet ($\sim 4 \times 10^7$ cells) was resuspended in 1 ml NP40 buffer (150 mM NaCl/1.5 mM $MgCl_2$/10 mM Tris, pH 7.4), centrifuged, and transferred into 400 μl NP40 buffer supplemented with 20 μl of 10 mM VRC. Cells were lysed by adding 50 μl of 10% NP40. The supernatant was transferred into 35 μl 143 mM EDTA (pH 8.0)/14% SDS, and then precipitated with 35 μl 3 M sodium acetate, 250 μl phenol and 250 μl chloroform. The aqueous phase was re-precipitated with 500 μl chloroform once and absolute ethanol twice. The obtained sample was stored as a slurry in 20 μl TE at −70°C. RNA was fractionated by electrophoresis in a denaturing 1% agarose gel. The samples were denatured at 68°C for 15 min and applied to a Zeta-Bind membrane (Bio-Rad) that had been equilibrated with 10 × SSC. Hybridization to a 1.3 kb gel-purified *Hin*dIII/*Xho*I restriction fragment of a c-*myc* cDNA clone that was labeled with [α-^{32}P]dCTP by random oligonucleotide priming was performed under aqueous conditions at 65°C. Blots were analyzed with a Molecular Dynamics PhosphorImager.

2.7. Detection of Myc protein

Cells were seeded at equal numbers into cell culture dishes and rendered quiescent by serum deprivation for 48 h in culture medium that contained only 0.25% fetal calf serum (FCS) instead of the normally used 10% FCS. The cells were stimulated to re-enter the active cell cycle by transfer into 10% FCS for a 4 h incubation period at 37°C. For the detection of Myc, the cells were washed three times in ice-cold phosphate-buffered saline (PBS), pelleted by centrifugation, re-suspended in lysis buffer containing the complete^{TM} serine and cysteine protease inhibitor cocktail from Boehringer, and solubilized in electrophoresis buffer (0.1 M Tris-HCl [pH 6.8], 4% SDS, 20% glycerol, 0.2% bromophenol blue). The amounts of total protein were determined by the Micro BCA method (Pierce) according to the manufacturer's specifications. Equal amounts of protein were fractionated by electrophoresis in 10% SDS/PAGE gels (Novex) and transferred to nitrocellulose (Schleicher and Schuell) by electroblotting for 1.5 h at 85 V in transfer buffer (0.2 M glycine, 20 mM Tris, 20% methanol). The blot was blocked by incubation for 1 h in Tris-buffered saline containing 5% skim milk and 0.05% Tween 20 (TBS-T), and then probed for 1 h at room temperature with 1 μg/ml of the "sc-764" rabbit anti-Myc polyclonal antiserum (Santa Cruz). Subsequently, the blot was incubated with a 1:2000 dilution of the peroxidase-conjugated secondary antibody "sc-2004" (Santa Cruz), which was raised against rabbit immunoglobulin. The chemiluminescence reagent from Pierce was used to develop the blot and visualize the Myc protein bands.

2.8. Determination of mutant frequencies

High molecular weight genomic DNA was prepared from TEPC 2372 after exposure to mutagens in vitro, using the Genomic DNA isolation kit from Qiagen. The DNA was solubilized in TE buffer (10 mM Tris, pH 8.0, 0.1 mM EDTA) and stored in the dark at 4°C. The λLIZ transgenes were recovered as infectious phages by mixing 6 μg genomic DNA adjusted to a concentration of 500 μg/ml with the Transpack packaging extract (Stratagene). Restriction-minus, recA, lacZΔM15 *E. coli* SCS-8 host cells were infected with recovered phage and plated out in top agarose containing 1.5 mg/ml X-gal. After incubation for 18 h at 37°C, the total number of plaques per plate was determined to assess the efficiency of phage packaging. It ranged usually from 6 to 48×10^3 plaques per packaging reaction. Blue plaques representing LacI$^-$ phages were carefully counted and then scored for mutant verification. To avoid the loss of those *lac*I mutants that expressed the phenotype of a very light blue color, the CM0 and CM1 faint color mutants (Stratagene) were used as internal sensitivity standards for the assay [28]. Mutant frequencies were calculated as the ratio of LacI$^-$ phage/total (LacI$^+$ + LacI$^-$) phage after treatment with model mutagens and

compared to the same ratio in the absence of such treatment. The latter reflected the background mutant frequency. The three mutagens used here, 4-NQO (4-nitroquinoline-1-oxide, Sigma), PhIP (2-hydroxyamino-1-methyl-6-phenylimidazo[4,5-b]pyridine, a gift from Dr. Elizabeth Snyderwine, NCI) and X/XO (xanthine/xanthine oxidase, Sigma), were added to exponentially growing TEPC 2372 cells for 2 or 24 h. The cells were washed three times in PBS (pH 7.4), resuspended in fresh culture medium, incubated for another 24 h in order to allow the premutagenic lesions to become fixed as mutations, and then harvested for the preparation of genomic DNA. According to the established Big Blue protocol, each sample was initially packaged in duplicates, but then recombined before the assay was completed. Some packaging reactions were performed in triplicates. 4-NQO was prepared as a 1 mM stock solution in DMSO. PhIP was stored as a 45 mM stock solution in DMSO and diluted to a 5 mM working solution in cell culture medium immediately before it was added to the cells. X/XO was freshly prepared as a 100× stock and added to the cell culture at final concentrations of 7 μg/ml and 15 μg/ml (∼0.08 units/ml), respectively.

3. Results

3.1. Derivation and properties of the plasmacytoma, TEPC 2372

TEPC 2372 was derived from a congenic BALB/c.λ LIZ$^{+/-}$ N_5 mouse that harbored a primary pristane-induced peritoneal plasmacytoma. The derivation of similar cell lines was attempted in parallel experiments from six additional plasmacytoma-bearing BALB/c.λ LIZ$^{+/-}$ N_5 mice, but was not successful. This poor result confirmed the past experience that establishing continuous cell lines from primary plasmacytomas is difficult without prior in vivo passaging of the tumors in pristane-primed BALB/c recipients [29]. The one cell line that was established was named "TEPC 2372" in reference to the tumor-inducing agent (2,6,10,14-tetramethylpentadecane is pristane), the nature of the tumor (plasmacytoma), and the number of the mouse (23–72) in which the tumor arose. During the first weeks of cell culture, the growth and survival of TEPC 2372 was strictly dependent on the presence of IL-6; however, an IL-6 independent subline was obtained later on by gradually weaning the cells from the growth factor. TEPC 2372 cells displayed the typical cytological features of a BALB/c plasmacytoma: large hyperchromatic and pleomorphic tumor cells that were further characterized by the basophilic cytoplasm, the paranuclear light zone, and the peculiar chromatin pattern in the nucleus (Fig. 1A). The tumor cells produced a γ2b heavy-chain/λlight-chain paraprotein, IgG2b/λ, of which substantial amounts were secreted into the cell culture supernatant (the 1:128,000 dilution of the proteins precipitated from the supernatant was still positive for γ2b in quantitative ELISA; results not shown). The γ2b phenotype is not uncommon among BALB/c plasmacytomas, although the majority (∼60%) of tumors produce IgA [18]. SSLP genotyping of TEPC 2372 revealed the presence of residual C57BL/6-derived alleles in two locations, the flank of the λLIZ transgene on Chr 4 and the proximal region of Chr 7 including the anonymous marker, D7MIT55.

Fig. 1. Morphology and cytogenetics of TEPC 2372. (A) Wsright's Giemsa-stained cytofuge specimen of malignant plasma cells in an early in vitro passage (original magnification, 40×). Binucleated tumor cells are indicated by arrows. (B) FISH mapping of the chromosomal integration site of the λLIZ transgene. Two fluorescence signals (one for each sister chromatid) were detected in the hyperdiploid subclone (see metaphase spread to the left) and four fluorescence signals were detected in the hypertetraploid subclone (see metaphase spread to the right). This was expected because the tumor is hemizygous for the λLIZ transgene (λLIZ$^{+/-}$). Chrs 4 that do not contain the transgene are also indicated by labeled arrows; one existed in the hyperdiploid subclone and two were detected in the hypertetraploid subclone. The inset, which displays a transgene-carrying Chr 4 together with a DAPI-stained image of the same chromosome and the chromosomal ideogram, illustrates the assignment of λLIZ to band C4-5. (C) Spectral karyotyping (SKY) revealed the presence of both products of the T(6;15) translocation. Two copies of the c-*myc*-deregulating product, Chr T(15;6), and one copy of the reciprocal product Chr T(6;15) were found. They are indicated by labeled arrows. (D) Comparative genomic hybridization (CGH). Shown are the CGH ratio profiles of those chromosomes that were characterized by loss or gain of genomic material. The corresponding metaphase chromosomes in SKY display and classification colors (presented as pairs with the display color to the left and the classification color to the right) are also shown to facilitate the understanding of the CGH profiles. See the third paragraph of the Section 3 for details.

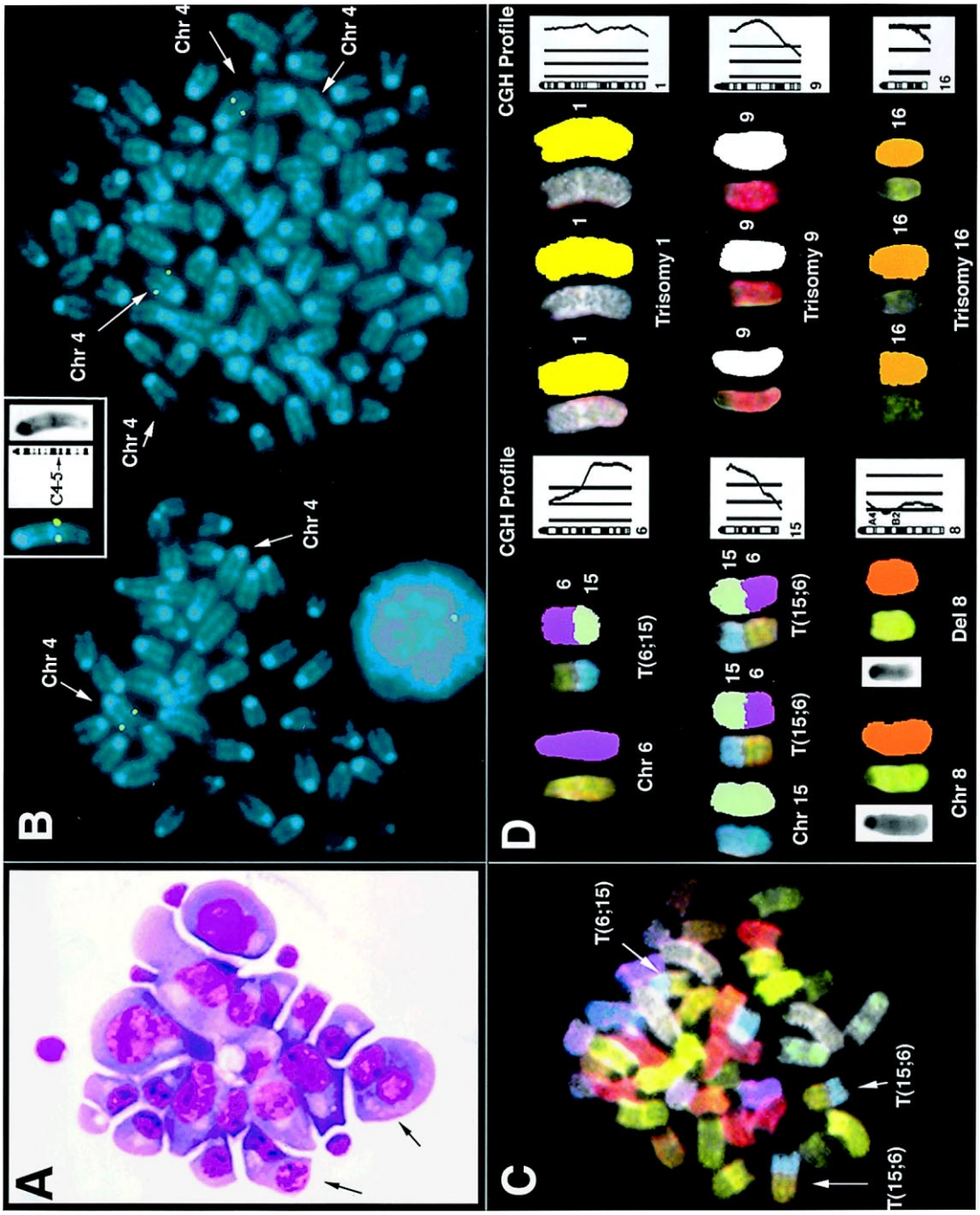
A
B
Chr 4
C4-5
Chr 4
Chr 4
Chr 4
Chr 4
Chr 4
C
T(6;15)
T(15;6)
T(15;6)
D
CGH Profile
6
15
Chr 6
T(6;15)
CGH Profile
1
1
1
Trisomy 1
15
6
15
6
Chr 15
T(15;6)
T(15;6)
9
9
9
Trisomy 9
Chr 8
Del 8
16
16
16
Trisomy 16

3.2. Chromosomal location and copy number of λLIZ

FISH was used to determine the chromosomal integration site of λLIZ in TEPC 2372. The comparison of the FISH-labeled with the DAPI-stained chromosome showed that the transgenic concatamer was inserted in the central portion of Chr 4 at band C4-5 (Fig. 1B). This location was compatible with the reported result of the genetic mapping to Tyrp1 [30], the gene encoding the tyrosine related protein that resides at 38 cM on the combined linkage map of Chr 4 (see http://www.informatics.jax.org). FISH analysis further revealed that TEPC 2372 was composed of two major subclones, a hyperdiploid one (∼40% of the cells) and a hypertetraploid one (∼60% of the cells). As expected for a tumor that originated in a hemizygous $\lambda LIZ^{+/-}$ mouse, one FISH signal was observed in the hyperdiploid population of TEPC 2372, and two were observed in the hypertetraploid population (cf. the two metaphase spreads in Fig. 1B). Quantitative Southern analysis demonstrated that approximately 59 copies of λLIZ were present in the genome of TEPC 2372 (Fig. 2). This number was significantly higher than expected, but the true copy number was still higher because of a correction for ploidy change according to the following consideration. Since parental, $\lambda LIZ^{+/+}$ homozygous Big Blue mice have been reported to contain approximately 80 copies of λLIZ, heterozygous $\lambda LIZ^{+/-}$ mice, which are diploid and contain 40 chromosomes, should harbor ∼40 copies of λLIZ. Furthermore, since TEPC 2372 is also $\lambda LIZ^{+/-}$ heterozygous, but hyperdiploid with a median chromosome number of 43 (see SKY and CGH data in the paragraph below), the apparent λLIZ copy number extrapolated from the blot shown in Fig. 2B (59 copies) needs to be normalized (i.e. multiplied) with the ratio between 43 and 40 (1.075), resulting in a total of ∼63 copies of λLIZ. It thus appears that TEPC 2372 contained 23 extra copies of the λLIZ transgene, presumably residing in the same single λLIZ concatamer that is present in the tumor line (see the above-mentioned FISH result). The putative amplification of λLIZ in situ may not be that surprising if one considers the many genetic changes that mark the history of the cell line (i.e. the backcross of λLIZ from C57BL/6 onto BALB/c, the malignant plasma cell transformation in mouse 23–72, and the establishment of the TEPC 2372 line in vitro).

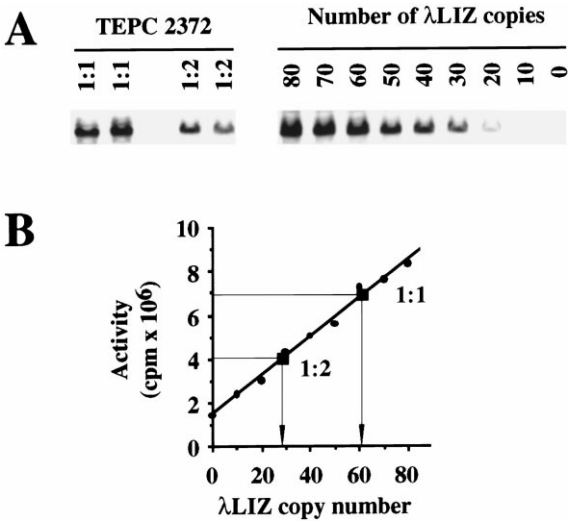

Fig. 2. Determination of λLIZ copy number by quantitative Southern blotting. Shown in panel A is the major, approximately 11 kb long Apa I fragment of the λLIZ transgene as detected in the plasmacytoma line (left panel labeled "TEPC 2372") and the parental C57BL/6 λLIZ homozygous ($\lambda LIZ^{+/+}$) Big Blue mouse (right panel labeled "number of λLIZ copies"). Two samples of TEPC 2372 were tested in duplicates: undiluted DNA from the IL-6 dependent line (pair of lanes labeled "1:1") and DNA from the IL-6 independent line after dilution with an equal amount of normal liver DNA (pair of lanes labeled "1:2"). Note that the fragment intensity of the 1:2 diluted sample is clearly weaker than that of the 1:1 sample. To generate the standard curve with which the number of λLIZ copies residing in TEPC 2372 could be determined, a serial dilution of Big Blue mouse DNA in λLIZ-free liver DNA was employed. The two DNAs were mixed at different ratios in order to blot 10–70 copies of λLIZ. Undiluted Big Blue DNA and normal liver DNA were used as end points defining 80 copies and zero copies of λLIZ, respectively. The intensity of the λLIZ fragments was determined by autoradiography, blotted graphically over the copy number of λLIZ (blue dots), and fitted by linear regression using the Cricket Graph software, as shown in panel B. The intensities of the λLIZ fragments in TEPC 2372 (red squares labeled "1:1" and "1:2") were used to extrapolate the apparent λLIZ copy number from the standard curve. Thus, approximately 28 copies were found in the 1:2 diluted tumor DNA (corresponding to 56 copies in the undiluted tumor DNA) and 62 copies were detected in the plain tumor sample. This resulted in the average copy number of 59, but after ploidy correction (see second paragraph of the Section 3) in the final copy number of 63.

3.3. Cytogenetics of TEPC 2372

A spectral karyotype that was typical of the hyperdiploid subclone of TEPC 2372 is displayed in Fig. 1C. The metaphase spread reveals the presence of both

products of the balanced chromosomal translocation, T(6;15). Two copies of the c-*myc*-deregulating product of translocation, Chr T(15;6), and one copy of the reciprocal product of translocation, Chr T(15;6), were found. The main findings of the CGH analysis are illustrated as CGH ratio profiles of those chromosomes for which apparent changes in gene-copy number were observed (Fig. 1D). Thus, Chrs 1, 9 and 16 occurred in triplets instead of pairs. The trisomies resulted in average CGH profiles that indicated gene amplification by being located to the right of the right-most vertical lines that are depicted next to the ideograms of Chrs 1, 9 and 16 (see insets labeled "CGH profile"). The close examination of the CGH profiles of Chrs 9 and 16 revealed the possibility that the extra copies of Chrs 9 and 16 were in fact incomplete towards their telomeric ends. This was suggested by the inward turn of the CGH profile curves in their distal portions; however, this interpretation requires further verification with cytogenetic methods that permit a better resolution than CGH. The presence of the additional, second copy of Chr T(15;6) led to the partial trisomy of both the distal half of Chr 6 and the centromeric half of Chr 15. This situation caused a shift to the right in the corresponding portions of the CGH profiles of Chrs 6 and 15. One allele of Chr 8 was detected to harbor a large deletion that appeared to span bands A4 and B2. This is indicated by the CGH profile of Chr 8, which was reflective of gene loss by crossing the left-most vertical line in the A4-B2 region. The reality that the deletion was monoallelic was confirmed when the size of the deleted copy of Chr 8 was compared with the size of the normal copy of Chr 8 after staining with DAPI (see small insets to the left of SKY-painted chromosomes) and painting with SKY (cf. the normal allele with the shortened allele in display color (green) and classification color (orange)).

3.4. Fine structure of the T(6;15) translocation

Chimeric junction fragments that included the genetic cross-over points and their flanking sequences were amplified by direct PCR and further determined by DNA sequencing (Fig. 3). The breaksites in the Pvt 1 gene and the 5′-Cκ region were accurately determined on both products of translocation, Chr T(6;15) and Chr T(15;6). Three interesting features of the translocation event were noted. First, the genetic exchange was nearly precise at the molecular level; i.e. it resulted in the loss of just 48 bp in Pvt 1 and no loss at all but a 16 bp duplication in the 5′-Cκ region (see underlined sequence, 5′-aaagaatgtagtttca-3′, in Fig. 3). Second, a 3 bp homology, 5′-tca-3′, was found at the breaksite on Chr T(6;15). Limited homologies of this sort have been observed frequently in breakpoint regions of T(12;15) translocations, which juxtapose a gene of the immunoglobulin heavy-chain gene cluster to c-*myc* [26,31,32], but the prevalence of microhomologies at T(6;15)-typical breaksites is not known because only a few cases have been elucidated at the DNA sequence level. Third, the genetic exchange on Chr T(15;6) was characterized by the existence of a 118 bp sequence that was inserted directly at the Pvt 1/5′-Cκ breaksite. The origin of the insert remains unknown, but its homology to the IMAGE cDNA clone 622552 (GenBank accession AI591913) suggested that it may have originated from an expressed gene. Similar insertions of incoming extraneous DNA have been detected previously in breakpoint regions of T(12;15) translocations [33].

3.5. Expression of c-myc

The expression of c-*myc* was determined under steady-state conditions at the mRNA level (Fig. 4) and under conditions of re-entry into the active cell cycle after relief from serum deprivation at the protein level (Fig. 5). Northern analysis (Fig. 4) demonstrated that TEPC 2372 contained c-*myc* RNA of 2.4 kb, the normal mature c-*myc* message that is known to contain exon 1, 2 and 3 sequences but no intronic sequences. The IL-6 dependent subline of TEPC 2372 (lanes 6 and 7) produced substantial amounts of the 2.4 kb message, nearly as much as the long-term established high-expression plasmacytoma, TEPC 1198 (lane 3), but the IL-6 independent subline clearly produced less (lane 5). TEPC 1198 is an appropriate control for TEPC 2372 because both tumors contain a T(6;15) translocation that, unlike the T(12;15), leaves the c-*myc* gene structurally intact [18]. To compare the activation of c-*myc* by virtue of the T(6;15) translocation with the activation of the gene in consequence of the more common T(12;15) translocation, two additional controls were included. The plasmacytoma MOPC 104E (lane 2), which harbors a T(12;15) that interrupts the c-*myc* gene in intron 1, expressed a

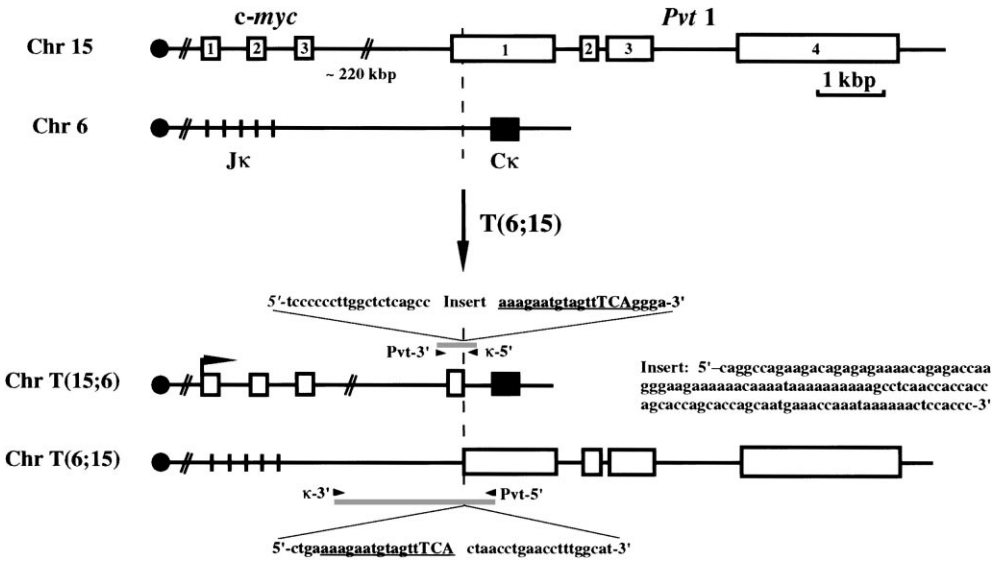

Fig. 3. Fine structure of the balanced T(6;15) chromosomal translocation detected in TEPC 2372. Shown in the top section are maps of the Pvt 1/c-*myc* megagene residing on Chr 15 and the Jκ/Cκ region located on Chr 6. The three exons of c-*myc* and the first four exons of Pvt 1 are designated by open boxes that are numbered. The Pvt 1 locus is located approximately 220 kbp downstream of the c-*myc* gene, as indicated by the oblique double line that is labeled. The Cκ exon is illustrated by a filled box labeled Cκ. The Jκ region, which contains five functional gene segments, is indicated by vertical lines marked Jκ. Centromeres are denoted by filled circles at the left end of chromosome maps. Chrs 6 and 15 are aligned at the postulated cross-over point of the T(6;15) translocation, which is indicated by a vertical dashed line. The genetic exchange took place in the first exon of Pvt 1 and the intervening sequence between Jκ and Cκ. Shown in the bottom section are structural schemata of the observed reciprocal recombination fragments produced by the T(6;15) translocation. Chr T(15;6) is critical for plasmacytomagenesis because it harbors the transcriptionally deregulated c-*myc* gene (indicated by the right-pointing arrow at the transcriptional start site of the gene at the beginning of exon 1) that encodes typically a 2.4 kb mRNA that consists of exon 1, 2, and 3 sequences. The two PCR junction fragments that were used for determining the translocation breakpoints by DNA sequencing are depicted by horizontal grey bars above and below the maps of Chrs T(15;6) and T(6;15), respectively. The annealing sites and designations of PCR primers are denoted by the labeled arrowheads. The sequences flanking the recombinational breaksites between Pvt 1 and Ck are shown (20 nucleotides in the 5′ and 3′ direction). Italics denote c-*myc* sequences and plain letters indicate 5′-Cκ sequences. The 16 bp duplication that was detected in the 5′-Cκ region (aaagaatgtagtttca) is underlined. It included the triplet, TCA, that was found exactly at the breaksite on Chr T(6;15). The triplet indicates a 3 bp microhomology at the cross-over point, since it could have been derived from both partners of recombination. It was arbitrarily assigned to Jκ. The DNA sequence of the 118 bp insert observed at the Pvt1/Cκ breaksite on Chr T(15;6) is specified to the right. See the fourth paragraph of the Section 3 for additional details.

decapitated c-*myc* message of 2.0 kb as the predominant molecular species [34]. The T(12;15)$^{+}$ plasmacytoma TEPC 2027E (lane 4) generated an atypically long 4.0 kb c-*myc* message, which is caused by the deletion of the splice donor site at the end of exon 1 [35]. Western analysis (Fig. 5) showed that the IL-6 independent subline of TEPC 2372 (lane 4) seemed to respond with a more vigorous expression of Myc than the IL-6 independent subline (lanes 5 and 6). This observation in conjunction with the above-mentioned result of Northern analysis raised the possibility that in TEPC 2372 the ability to upregulate Myc protein may be inversely related to the steady-state level of c-*myc* mRNA. However, this hypothesis requires further proof. Myc expression in TEPC 2372 was further compared to the fibroblast line, HO15.19, that was engineered by Dr. John Sedivy (Brown University) to contain two null alleles of c-*myc* (loss of protein expression), and a derivative thereof, TGR-1, that was re-constituted for Myc expression [36]. As expected, TGR-1 cells produced the 62 kD Myc protein, whereas HO15.19 did not. The combined results of Northern and Western analysis demonstrated that Myc is constitutively expressed in TEPC 2372.

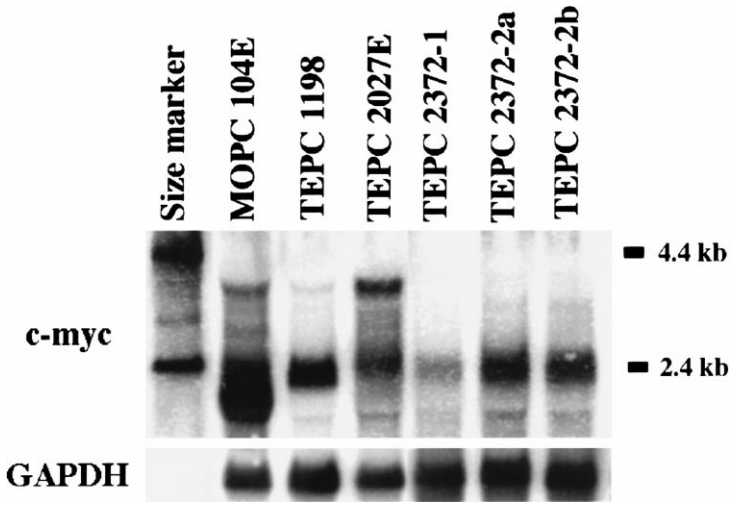

Fig. 4. Analysis of c-*myc* RNA content. A total amount of 5 μg RNA from TEPC 2372 and three additional BALB/c plasmacytomas (MOPC 104E, TEPC 1198, TEPC 2027E) was electrophored through a 1% denaturing agarose gel and blotted onto a nitrocellulose membrane. The blot was first probed with nick-translated c-*myc* cDNA (1.3 kb *Hin*dIII/*Xho*I fragment) that included the protein-encoding exons 2 and 3 and after stripping re-probed with a cDNA probe for the housekeeping gene, GAPDH. Note that the IL-6 independent subline of TEPC 2372 (sample TEPC 2372-1) appeared to express lower steady-state amounts of c-*myc* message than the IL-6 dependent subline (samples TEPC 2372-2a/b).

3.6. Mutagenicity testing with early passage cells

A pilot experiment with early-passage plasmacytoma cells (see first paragraph of the Section 2 for definition of "early passage") was performed to demonstrate the principal utility of TEPC 2372 for evaluating mutagenesis in vitro and to justify additional efforts to develop a stable cell line. To determine the background mutant rate of λLIZ in TEPC 2372, DNA obtained from untreated tumor cells was packaged in three separate packaging reactions and pooled prior to performing the λLIZ assay. The combined results of two independent experiments (i.e. six packaging reactions) revealed the acceptable spontaneous mutant frequency of 8.23×10^{-5}. To evaluate the ability of TEPC 2372 to undergo induced mutagenesis, the cells were challenged with the model mutagens 4-NQO, PhIP, and X/XO. 4-NQO is a UV-mimetic mutagen that is believed to exert significant genotoxic potential via the generation of reactive oxygen species [37,38]. X/XO is a substrate/enzyme system that generates a flux of the reactive oxygen species, superoxide anion and hydrogen peroxide [39]. PhIP is a heterocyclic amine that forms promutagenic DNA lesions via adduct formation with guanine [40,41]. Table 1 (Experiment 1) shows that the exposure of TEPC 2372 to the above-mentioned mutagens resulted in significant increases in λLIZ mutant levels over the background mutant frequency, namely 6.55-fold after challenge with 4-NQO (1 μM), 3.39-fold after challenge with X/XO, and 5.11-fold after challenge with PhIP (when the results at exposure levels of 1 and 2 μM were combined).

3.7. Mutagenicity testing with the established cell line

Two experiments with the established TEPC 2372 line (see first paragraph of the Section 2 for definition of "established") were conducted to assess the mutagenicity of 4-NQO in greater detail (Table 1). The assessment, which was based on screening a total number of 3.66×10^6 plaques in Experiment 2 and 2.07×10^6 plaques in Experiment 3, produced the following results. First, the spontaneous or background mutant frequency in untreated established tumor cells appeared to be significantly increased (14.8×10^{-5} on average) when compared to early-passage cells (8.3×10^{-5} on average). This increase by approximately

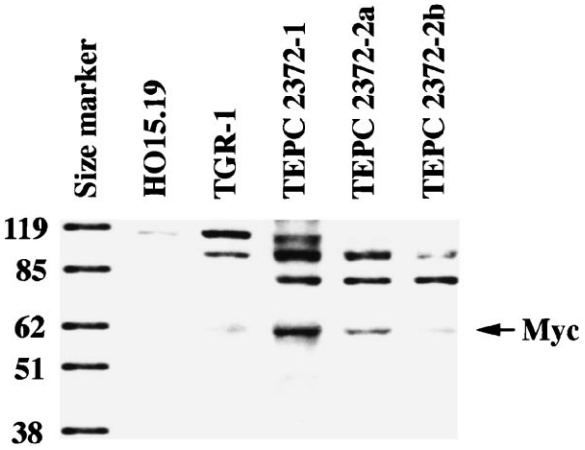

Fig. 5. Determination of Myc protein content in TEPC 2372. A total amount of 10 μg protein obtained from TEPC 2372 and two fibroblast lines, HO15.19 and TGR-1, was electrophored through a 10% SDS/PAGE gel and blotted onto a nitrocellulose membrane. The blot was probed with a rabbit anti-Myc antiserum followed by a peroxidase-labeled antibody with specificity against rabbit immunoglobulins, then developed by chemiluminescence. The band for Myc is indicated by an arrow that is labeled. All other bands are artifacts, including the approximately 80 kD band that is present in all lanes of TEPC 2372. The 80 kD band may have been due to the binding of the endogenous IgG2b paraprotein by the secondary antiserum (anti-rabbit Ig with presumable cross-reactivity to mouse IgG) that was used to probe the blot, but this has not been demonstrated. Note that two sublines of TEPC 2372 were tested: TEPC 2372-1, the IL-6 independent subline (lane 4) and TEPC 2372-2a/b, the IL-6 dependent subline (lanes 5 and 6). HO15.19 and TGR-1 were used as negative and positive controls for Myc expression, respectively. HO15.19 has been genetically disabled to express Myc, whereas the derivative line, TGR-1, has been reconstituted for Myc expression [36]. The two fibroblast lines were a generous gift from Dr. John Sedivy, Brown University. Note that the IL-6 independent subline of TEPC 2372 (sample TEPC 2372-1) appeared to express higher levels of Myc upon re-entry into the active cell cycle than the IL-6 dependent subline (samples TEPC 2372-2a/b).

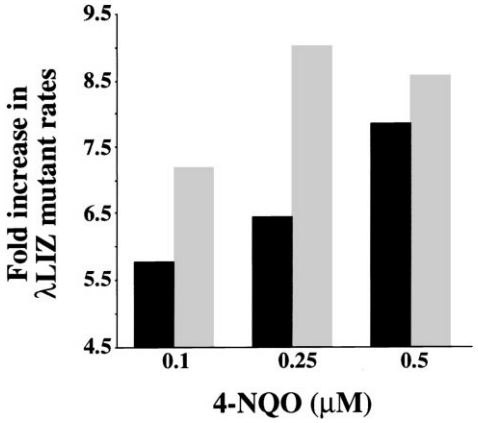

Fig. 6. Enhancement of 4-NQO-induced mutagenesis by BSO. TEPC 2372 was challenged with 4-NQO (black bars) or 4-NQO plus 10 μM BSO (grey bars) as described in the Section 2. The fold increase in λLIZ mutant rates was calculated by dividing the mutant frequency after challenge with mutagen by the corresponding background mutant frequency, 16.2×10^{-5} in Experiment 2 and 12.0×10^{-5} in Experiment 3. BSO caused an apparent increase in λLIZ mutant rates of 25, 40, and 9% at 4-NQO concentrations of 0.1, 0.25, and 0.5 μM, respectively. See Table 1 and the last paragraph of the Section 3 for further details.

80% must have occurred during the 6-month consolidation period of the cell line in vitro, possibly reflecting the accumulation of genetic alterations that relaxed genomic stability control and/or the action of c-*myc* as a mutator gene (see last paragraph of the Section 4 for this speculation). Second, although elevations of spontaneous mutant frequencies result inevitably in the tendency to suppress dose-response curves of mutagens, TEPC 2372 was still found to respond to 4-NQO with a vigorous dose-dependent increase in mutant frequencies, demonstrating a peak 7.85-fold increase at a concentration of 0.5 μM 4-NQO (Experiment 2). Third, cotreatment of TEPC 2372 with the same dose range of 4-NQO plus a constant amount of BSO (10 μM) resulted in a somewhat higher elevation of mutant rates (9.03-fold increase) observed at a lower concentration of 4-NQO (0.25 μM). BSO, which effects the depletion of intracellular glutathione stores by inhibiting its biosynthesis, is known to increase endogenous oxidative stress. This observation and the finding that BSO added to the general toxicity of 4-NQO (phage packaging collapsed at 1.0 μM 4-NQO in Experiment 2, but at 0.75 μM 4-NQO in Experiment 3) raised the possibility that BSO may synergize with the oxidative mutagenesis induced by 4-NQO (Fig. 6). Taken together, the results of the mutagenicity experiments proved that the λLIZ assay was reliably reporting mutation events in TEPC 2372.

4. Discussion

The Big Blue mouse in vivo mutagenesis system™ (Stratagene) is based on the phage λ-derived transgenic shuttle vector λLIZ, which contains genes *lac*I

and αlacZ as target and reporter genes of mutagenesis. Our main goal in employing the λLIZ assay is to gain further insights into experimental plasmacytomagenesis in mice. We are particularly interested in analyzing the oxidative mutations that appear to accumulate in the mature B-cell lineage during plasmacytoma development [21,42] and to identify the genes that control this phenotype. Plasmacytomas are malignant tumors that correspond to terminally differentiated B cells, plasma cells. They can be readily induced in the peritoneal cavity of genetically susceptible BALB/c mice by i.p. injections of inflammatory agents, such as pristane [43] or silicone polymers [44]. Since peritoneal plasmacytomagenesis in mice depends on the genotype of BALB/c, we decided to backcross the C57BL/6-derived λLIZ transgene onto BALB/c in order to develop a syngeneic system in which plasmacytoma development can be associated with oxidative B-cell mutagenesis. Prior to completing the backcross, we chose to carry out a tumor induction experiment to prove that the backcross of the approximately 1.8 Mbp long λLIZ concatamer did not abolish the susceptibility of strain BALB/c to undergo plasmacytomagenesis. This experiment was conducted in mice from the fifth backcross generation (N_5), which were — with the exception of some C57BL/6-derived alleles flanking the transgene on Chr 4 and other alleles residing in the centromeric region of Chr 7 — genetically pure (congenic) and hemizygous for λLIZ (BALB/c.λLIZ$^{+/-}$ N_5 mice). The plasmacytoma cell line described here, TEPC 2372, was derived from one of the plasmacytomas that developed in BALB/c.λLIZ$^{+/-}$ N_5 mice.

TEPC 2372 seems to be a typical BALB/c plasmacytoma by various accounts (paraprotein production, c-*myc*-activating chromosomal translocation, initial dependence on IL-6 ...), but is also characterized by the unusual property of being able to report mutagenesis after in vitro exposure to oxidative agents. This feature should make it a useful addition to the two λLIZ-containing cell lines that have been developed previously, the Rat2.λLIZ embryo fibroblasts [45] and the Big Blue mouse embryo fibroblasts (not published yet, but described in Stratagene's newsletter "Strategies", volume 10, number 1, 1997). Rat2.λLIZ fibroblasts have already been validated in mutagenicity studies in which the cells were exposed to the alkylating agent *N*-methyl-*N*-nitrosurea (MNU) [45], the butadiene metabolite 1,2:3,4-diepoxybutane [46], the polycyclic carcinogen 7,12-dimethylbenz[a]anthracene [47], the plasmacytomagenic C_{19}-alkane pristane [48], and the small siloxane tetravinyl-D4 [49]. These studies have clearly established that Rat2.λLIZ fibroblasts are practical for assessing mutagenicity in vitro, but they have also demonstrated that the utility of the line is somewhat limited by its nature as a stable transfectant of λLIZ. This reflects itself in two ways. First, the fibroblasts harbor only approximately 60 copies of the λLIZ shuttle vector instead of the 80 copies present in homozygous λLIZ$^{+/+}$ transgenic mice. Second, and more important, since the shuttle vector has been inserted in two different, unidentified locations of the fibroblast genome, potential positional effects cannot be ruled out when the mutant rates of the transfected λLIZ are compared with those of the transgenic counterpart. Big Blue mouse embryo fibroblasts, which contain the λLIZ transgene at the same copy number and chromosomal location as the transgenic mice, may promise a more authentic in vitro equivalent of the λLIZ in vivo mutagenesis assay, yet this will have to be demonstrated in validation studies. TEPC 2372 plasmacytoma cells are similar to Big Blue fibroblasts in that they harbor λLIZ at the same chromosomal location as the transgenic mice.

We believe that TEPC 2372 may be helpful to further our understanding of the role of oxidative mutagenesis in mouse plasma cell tumor development. Two experiments shall be briefly mentioned to illustrate this point. First, a number of congenic mouse strains have been developed recently that are distinguished by both the presence of DBA/2N-derived plasmacytoma resistance genes on the BALB/c background and differences in the susceptibility to plasmacytomagenesis [50]. These strains may additionally display genotypic differences in oxidative B-cell mutagenesis; however, the differences may be relatively small and only detectable after challenging the mice with a carefully selected mutagen. We hypothesize that TEPC 2372 may assist in identifying suitable candidate mutagens and aid, thereby, in the design of the most effective in vivo study. Second, recent evidence suggests that the constitutive expression of Myc may effect a cellular phenotype that is of great interest to cancer research, increased genomic instability [51]. Myc-induced genomic instability has been demonstrated to take the form of amplification of growth-related genes in

BALB/c plasmacytomas [52–54], and ploidy changes and chromosomal aberrations in both mammary carcinomas [55] and primary fibroblasts [56]. We submit that TEPC 2372 may be useful for testing another aspect of the "Myc-as-mutator-gene hypothesis", namely the possibility that deregulated Myc may increase general mutagenesis. Experimental conditions could be chosen to elevate or reduce Myc levels in the tumor line to test how this might affect the mutant frequency in λLIZ. Transfection with inducible Myc expression vectors [57] could be used to upregulate Myc, and transfection with vectors expressing dominant negative forms of Max [58] or members of the Myc inhibitory network [59] could be used to downregulate Myc. These experiments, which have been encouraged by a recent report that overexpression of Myc in the liver resulted in elevated levels of liver mutagenesis [40], are in progress in our laboratory.

Acknowledgements

We are grateful to Drs. Michael Potter and J. Frederick Mushinski for many insightful discussions in the course of the experiments, reading the manuscript, and making helpful suggestions for its improvement. We acknowledge Wendy DuBois for animal husbandry, Dr. Beverly Mock for advice on genotyping, Dr. J. Frederick Mushinski for providing mRNA samples and help with Northern blotting, Nicole McNeil for making available reference slides for CGH, Dr. Konrad Huppi for advice on PCR primer selection and the kind gift of primers Pvt-5′ and κ-3′, Dr. John Sedivy for the generous gift of the fibroblast lines HO15.19 and TGR-1, and Dr. Elizabeth G. Snyderwine for the mutagen PhIP. These studies were supported in part by a grant to Dr. G.-W. Bornkamm from the Mildred-Scheel-Stiftung for cancer research.

References

[1] T. Nohmi, M. Katoh, H. Suzuki, M. Matsui, M. Yamada, M. Watanabe, M. Suzuki, N. Horiya, O. Ueda, T. Shibuya, H. Ikeda, T. Sofuni, A new transgenic mouse mutagenesis test system using Spi- and 6-thioguanine selections, Environ. Mol. Mutagen. 28 (1996) 465–470.

[2] J.G. Burkhart, H.V. Malling, Mutagenesis and transgenic systems: perspective from the mutagen, *N*-ethyl-*N*-nitrosourea, Environ. Mol. Mutagen. 22 (1993) 1–6.

[3] E.G. Leach, L. Narayanan, P.A. Havre, E.J. Gunther, T.M. Yeasky, P.M. Glazer, Tissue specificity of spontaneous point mutations in lambda supF transgenic mice, Environ. Mol. Mutagen. 28 (1996) 459–464.

[4] Y. Gondo, Y. Shioyama, K. Nakao, M. Katsuki, A novel positive detection system of in vivo mutations in rpsL (strA) transgenic mice, Mutat. Res. 360 (1996) 1–14.

[5] J.A. Gossen, W.J. de Leeuw, C.H. Tan, E.C. Zwarthoff, F. Berends, P.H. Lohman, D.L. Knook, J. Vijg, Efficient rescue of integrated shuttle vectors from transgenic mice: a model for studying mutations in vivo, Proc. Natl. Acad. Sci. U.S.A. 86 (1989) 7971–7975.

[6] S.W. Dean, B. Myhr, Measurement of gene mutation in vivo using Muta Mouse and positive selection for lacZ-phage, Mutagenesis 9 (1994) 183–185.

[7] S.W. Kohler, G.S. Provost, A. Fieck, P.L. Kretz, W.O. Bullock, D.L. Putman, J.A. Sorge, J.M. Short, Analysis of spontaneous and induced mutations in transgenic mice using a lambda ZAP/*lac*I shuttle vector, Environ. Mol. Mutagen. 18 (1991) 316–321.

[8] J.L. Jakubczak, G. Merlino, J.E. French, W.J. Muller, B. Paul, S. Adhya, S. Garges, Analysis of genetic instability during mammary tumor progression using a novel selection-based assay for in vivo mutations in a bacteriophage lambda transgene target, Proc. Natl. Acad. Sci. U.S.A. 93 (1996) 9073–9078.

[9] M.E. Boerrigter, M.E. Dolle, H.J. Martus, J.A. Gossen, J. Vijg, Plasmid-based transgenic mouse model for studying in vivo mutations, Nature 377 (1995) 657–659.

[10] L. Recio, L.J. Pluta, K.G. Meyer, The in vivo mutagenicity and mutational spectrum at the *lac*I transgene recovered from the spleens of B6C3F1 *lac*I transgenic mice following a 4-week inhalation exposure to 1,3-butadiene, Mutat. Res. 401 (1998) 99–110.

[11] S.C. Sisk, L.J. Pluta, J.A. Bond, L. Recio, Molecular analysis of *lac*I mutants from bone marrow of B6C3F1 transgenic mice following inhalation exposure to 1,3-butadiene, Carcinogenesis 15 (1994) 471–477.

[12] M.G. Manjanatha, S.D. Shelton, A. Aidoo, L.E. Lyn-Cook, D.A. Casciano, Comparison of in vivo mutagenesis in the endogenous Hprt gene and the *lac*I transgene of Big Blue(R) rats treated with 7,12-dimethylbenz[a]anthracene, Mutat. Res. 401 (1998) 165–178.

[13] A.H. Mullin, R. Rando, F. Esmundo, D.A. Mullin, Inhalation of benzene leads to an increase in the mutant frequencies of a *lac*I transgene in lung and spleen tissues of mice, Mutat. Res. 327 (1995) 121–129.

[14] T.R. Skopek, K.L. Kort, D.R. Marino, Relative sensitivity of the endogenous hprt gene and *lac*I transgene in ENU-treated Big Blue B6C3F1 mice, Environ. Mol. Mutagen. 26 (1995) 9–15.

[15] A. Hakura, Y. Tsutsui, J. Sonoda, J. Kai, T. Imade, M. Shimada, Y. Sugihara, T. Mikami, Comparison between in vivo mutagenicity and carcinogenicity in multiple organs by benzo[a]pyrene in the lacZ transgenic mouse (Muta mouse), Mutat. Res. 398 (1998) 123–130.

[16] E.J. Mientjes, A. Luiten-Schuite, E. van der Wolf, Y. Borsboom, A. Bergmans, F. Berends, P.H. Lohman, R.A.

Baan, J.H. van Delft, DNA adducts, mutant frequencies, and mutation spectra in various organs of lambda lacZ mice exposed to ethylating agents, Environ. Mol. Mutagen. 31 (1998) 18–31.
[17] C.V. Williams, K. Fletcher, H. Tinwell, J. Ashby, Mutagenicity of ethyl carbamate to lacZ-transgenic mice, Mutagenesis 13 (1998) 133–137.
[18] M. Potter, F. Wiener, Plasmacytomagenesis in mice: model of neoplastic development dependent upon chromosomal translocations, Carcinogenesis 13 (1992) 1681–1697.
[19] R.P. Nordan, M. Potter, A macrophage-derived factor required by plasmacytomas for survival and proliferation in vitro, Science 233 (1986) 566–569.
[20] T.H. Yosida, H.T. Imai, M. Potter, Chromosomal alteration and development of tumors. XIX. Chromosome constitution of tumor cells in 16 plasma cell neoplasms of BALB-c mice, J. Natl. Cancer Inst. 41 (1968) 1083–1097.
[21] K. Felix, K.A. Kelliher, G.W. Bornkamm, S. Janz, Elevated mutant frequencies in lymphoid tissues persist throughout plasmacytoma development in BALB/c.lambdaLIZ mice, Cancer Res. 59 (1999) 3621–3626.
[22] M. Liyanage, A. Coleman, S. du Manoir, T. Veldman, S. McCormack, R.B. Dickson, C. Barlow, A. Wynshaw-Boris, S. Janz, J. Wienberg, M.A. Ferguson-Smith, E. Schröck, T. Ried, Multicolour spectral karyotyping of mouse chromosomes, Nat. Genet. 14 (1996) 312–315.
[23] A.E. Coleman, E. Schröck, Z. Weaver, S. du Manoir, F. Yang, M.A. Ferguson-Smith, T. Ried, S. Janz, Previously hidden chromosome aberrations in T(12;15)-positive BALB/c plasmacytomas uncovered by multicolor spectral karyotyping, Cancer Res. 57 (1997) 4585–4592.
[24] A. Coleman, S. Forest, N. McNeil, A. Kovalchuk, T. Ried, S. Janz, Cytogenetic analysis of the bipotential murine pre-B cell lymphoma, P388, and its derivative macrophage-like tumor, P388D1, using SKY and CGH, Leukemia 13 (1999) 1592–1600.
[25] B.A. Mock, L.A. D'Hoostelaere, R. Matthai, K. Huppi, A mouse homeo box gene Hox-1.5, and the morphological locus, Hd, map to within 1 cM on chromosome 6, Genetics 116 (1987) 607–612.
[26] J.R. Müller, M. Potter, S. Janz, Differences in the molecular structure of c-*myc*-activating recombinations in murine plasmacytomas and precursor cells, Proc. Natl. Acad. Sci. U.S.A. 91 (1994) 12066–12070.
[27] A.L. Kovalchuk, J.R. Müller, S. Janz, Deletional remodeling of c-*myc*-deregulating translocations, Oncogene 15 (1997) 2369–2377.
[28] B.J. Rogers, G.S. Provost, R.R. Young, D.L. Putman, J.M. Short, Intralaboratory optimization and standardization of mutant screening conditions used for a lambda/*lac*I transgenic mouse mutagenesis assay (I), Mutat. Res. 327 (1995) 57–66.
[29] M. Potter, J.G. Pumphrey, J.L. Walters, Growth of primary plasmacytomas in the mineral oil-conditioned peritoneal environment, J. Natl. Cancer Inst. 49 (1972) 305–308.
[30] M.J. Dycaico, G.S. Provost, P.L. Kretz, S.L. Ransom, J.C. Moores, J.M. Short, The use of shuttle vectors for mutation analysis in transgenic mice and rats, Mutat. Res. 307 (1994) 461–478.
[31] J.R. Müller, G.M. Jones, M. Potter, S. Janz, Detection of immunoglobulin/c-*myc* recombinations in mice that are resistant to plasmacytoma induction, Cancer Res. 56 (1996) 419–423.
[32] J.R. Müller, S. Janz, M. Potter, Differences between Burkitt's lymphomas and mouse plasmacytomas in the immunoglobulin heavy chain/c-*myc* recombinations that occur in their chromosomal translocations, Cancer Res. 55 (1995) 5012–5018.
[33] J.R. Müller, G.M. Jones, S. Janz, M. Potter, Migration of cells with immunoglobulin/c-*myc* recombinations in lymphoid tissues of mice, Blood 89 (1997) 291–296.
[34] J.F. Mushinski, c-*myc* Oncogene activation and chromosomal translocation in BALB/c plasmacytomas, in: G. Klein (Ed.), Cellular Oncogene Activation, Marcel Dekker, New York, 1988, pp. 181–222.
[35] S.R. Bauer, M. Piechaczyk, R.P. Nordan, J.D. Owens, A. Nepveu, K.B. Marcu, J.F. Mushinski, Altered Myc gene transcription and intron-induced stabilization of Myc RNAs in two mouse plasmacytomas, Oncogene 4 (1989) 615–623.
[36] M.K. Mateyak, A.J. Obaya, S. Adachi, J.M. Sedivy, Phenotypes of c-Myc-deficient rat fibroblasts isolated by targeted homologous recombination, Cell Growth. Differ. 8 (1997) 1039–1048.
[37] T. Nunoshiba, B. Demple, Potent intracellular oxidative stress exerted by the carcinogen 4-nitroquinoline-1-oxide, Cancer Res. 53 (1993) 3250–3252.
[38] D. Ramotar, E. Belanger, I. Brodeur, J.Y. Masson, E.A. Drobetsky, A yeast homologue of the human phosphotyrosyl phosphatase activator PTPA is implicated in protection against oxidative DNA damage induced by the model carcinogen 4-nitroquinoline 1-oxide, J. Biol. Chem. 273 (1998) 21489–21496.
[39] R. Zimmerman, P. Cerutti, Active oxygen acts as a promoter of transformation in mouse embryo C3H/10T1/2/C18 fibroblasts, Proc. Natl. Acad. Sci. U.S.A. 81 (1984) 2085–2087.
[40] C.D. Davis, E.J. Dacquel, H.A. Schut, S.S. Thorgeirsson, E.G. Snyderwine, In vivo mutagenicity and DNA adduct levels of heterocyclic amines in Muta mice and c-*myc*/lacZ double transgenic mice, Mutat. Res. 356 (1996) 287–296.
[41] L. Fan, H.A. Schut, E.G. Snyderwine, Cytotoxicity, DNA adduct formation and DNA repair induced by 2-hydroxyamino-3-methylimidazo[4,5-f]quinoline and 2-hydroxyamino-1-methyl-6-phenylimidazo[4,5-b]pyridine in cultured human mammary epithelial cells, Carcinogenesis 16 (1995) 775–779.
[42] K. Felix, K. Kelliher, G.W. Bornkamm, S. Janz, Association of elevated mutagenesis in the spleen with genetic susceptibility to induced plasmacytoma development in mice, Cancer Res. 58 (1998) 1616–1619.
[43] P.N. Anderson, M. Potter, Induction of plasma cell tumours in BALB-c mice with 2,6,10,14-tetramethylpentadecane (pristane), Nature 222 (1969) 994–995.
[44] M. Potter, S. Morrison, F. Wiener, X.K. Zhang, F.W. Miller, Induction of plasmacytomas with silicone gel in genetically susceptible strains of mice, J. Natl. Cancer Inst. 86 (1994) 1058–1065.

[45] D.L. Wyborski, S. Malkhosyan, J. Moores, M. Perucho, J.M. Short, Development of a rat cell line containing stably integrated copies of a lambda/*lac*I shuttle vector, Mutat. Res. 334 (1995) 161–165.
[46] C.J. Saranko, L. Recio, The butadiene metabolite 1,2:3,4-diepoxybutane, induces micronuclei but is only weakly mutagenic at *lac*I in the Big Blue Rat2 *lac*I transgenic cell line, Environ. Mol. Mutagen. 31 (1998) 32–40.
[47] M.G. Manjanatha, J.B. Chen, J.G. Shaddock Jr., A.J. Harris, S.D. Shelton, D.A. Casciano, Molecular analysis of *lac*I mutations in Rat2 cells exposed to 7,12-dimethylbenz[a]anthracene: evidence for DNA sequence and DNA strand biases for mutation, Mutat. Res. 372 (1996) 53–64.
[48] K. Felix, M. Potter, G.W. Bornkamm, S. Janz, In vitro mutagenicity of the plasmacytomagenic agent pristane (2,6,10,14-tetramethylpentadecane), Cancer Lett. 113 (1997) 71–76.
[49] K. Felix, S. Lin, G.W. Bornkamm, S. Janz, Tetravinyltetramethylcyclo-tetrasiloxane (tetravinyl D4) is a mutagen in Rat2lambda *lac*I fibroblasts, Carcinogenesis 19 (1998) 315–320.
[50] B.A. Mock, J. Hartley, P. Le Tissier, J.S. Wax, M. Potter, The plasmacytoma resistance gene Pctr2, delays the onset of tumorigenesis and resides in the telomeric region of chromosome 4, Blood 90 (1997) 4092–4098.
[51] L.A. Loeb, Mutator phenotype may be required for multistage carcinogenesis, Cancer Res. 51 (1991) 3075–3079.
[52] S. Mai, J. Hanley-Hyde, M. Fluri, c-Myc overexpression associated DHFR gene amplification in hamster, rat, mouse and human cell lines, Oncogene 12 (1996) 277–288.
[53] S. Mai, M. Fluri, D. Siwarski, K. Huppi, Genomic instability in MycER-activated Rat1A-MycER cells, Chromosome Res. 4 (1996) 365–371.
[54] S. Mai, Overexpression of c-*myc* precedes amplification of the gene encoding dihydrofolate reductase, Gene 148 (1994) 253–260.
[55] S.J. McCormack, Z. Weaver, S. Deming, G. Natarajan, J. Torri, M.D. Johnson, M. Liyanage, T. Ried, R.B. Dickson, Myc/p53 interactions in transgenic mouse mammary development, tumorigenesis and chromosomal instability, Oncogene 16 (1998) 2755–2766.
[56] D.W. Felsher, J.M. Bishop, Transient excess of MYC activity can elicit genomic instability and tumorigenesis, Proc. Natl. Acad. Sci. U.S.A. 96 (1999) 3940–3944.
[57] M. Eilers, D. Picard, K.R. Yamamoto, J.M. Bishop, Chimaeras of Myc oncoprotein and steroid receptors cause hormone-dependent transformation of cells, Nature 340 (1989) 66–68.
[58] D. Krylov, K. Kasai, D.R. Echlin, E.J. Taparowsky, H. Arnheiter, C. Vinson, A general method to design dominant negatives to B-HLHZip proteins that abolish DNA binding, Proc. Natl. Acad. Sci. U.S.A. 94 (1997) 12274–12279.
[59] D.E. Ayer, L. Kretzner, R.N. Eisenman, Mad: a heterodimeric partner for Max that antagonizes Myc transcriptional activity, Cell 72 (1993) 211–222.